Maximum Loadability Assessment of the Nigerian 330kv Transmission Network Using P-V Curve Method

CHRISTOPHER O. AHIAKWO[1], DIKIO C. IDONIBOYEOBU[2], SEPIRIBO L. BRAIDE[3], CHUKWUKA L. ONITA[4]

[1, 2, 3, 4] *Electrical Engineering Department, Rivers State University*

Abstract- System operating limits are usually based upon certain operating criteria though they are not limited to the following: Facility ratings**,** Voltage stability ratings**,** Transient stability ratings and System voltage limits. All components in the Nigerian 330KV transmission network operate between predefined limits in normal condition and the technical operational thresholds for power systems involve physical and system theoretical. Newton-Rapson load flow method was used to determine optimal location for static var placement. 5 buses were identified and compensated using NEPLAN Software for the system modeling. P-V curve plot showcased the maximum loading of the system {operating margin). P-V curve comparison for pre-upgrade, post-upgrade and artificial neural network respectively in respect to the 5 buses was plotted. For Gombe bus, the red curve indicates the maximum loadability of the pre-upgrade network at 700MW. The green curve indicates the effect of static var compensation with maximum loadability at 1100MW. Therefore, the improvement achieved is 400MW. Finally, the artificial neural network technique is represented by the blue curve and it validated the improvement achieved as the voltage and real power remain fairly constant with static compensators. For Jalingo bus, the red curve maximum loadability is at 550MW. The green curve maximum loadability is at 1150MW. Finally, the blue curve validated the improvement achieved. For Yola bus, the maximum loadability is at 620MW. The green curve maximum loadability is at 1100MW. Finally, the blue curve validated the improvement achieved. For Maiduguri bus, the red curve maximum loadability is at 600MW. The green curve maximum loadability is at 1120MW. Finally, the blue curve validated the improvement achieved. For Damaturu bus, the red curve maximum loadability is at 450MW while the green curve maximum loadability is at 1150MW meaning about 650MW improvement was achieved.

I. INTRODUCTION

The Nigerian 330KV transmission network is the highest bulk power transfer in Nigeria grid system managed by Nigerian Transmission Company. The Nigeria national grid system is an interconnection of 9,454km length of 330KV transmission line made of 22 generating stations through a network of fifty-nine (59) buses and sixty-seven (67) transmission lines of either dual or single circuit lines with 48 load buses and four control centers (one national control center at Oshogbo and three supplementary control centers at Benin, Shiroro and Egbin). The Nigeria 330KV transmission network covers a total length of 9,454km with total installed transformer capacity of 7688MVA and average available capacity of 7364MVA. (Ezekiel, *et al.,* 2019)

A system operating limit is defined as the value (such as MW, MVar, Amperes, Frequency or Volts) that satisfies the most limiting of the prescribed operating criteria for a specified system configuration to ensure operation within acceptable reliability criteria. System operating limits are usually based upon certain operating criteria though they are not limited to the following: Facility ratings (applicable pre- and post-contingency equipment or facility rating)**,** Voltage stability ratings (applicable pre- and/or post-contingency voltage stability) and Transient stability ratings (applicable pre- and/or post- contingency stability limits) and System voltage limits (applicable pre- and post- contingency voltage limits). All components operate between predefined limits in normal condition and the technical operational thresholds for power systems involve physical and system theoretical (Ademola, *et al.,* 2016).

For the power system operational safety and stable power transfer across Nigerian 330kv transmission system without violating any operating limit, it's imperative for operating limit monitoring by efficient tools for the voltage stability assessment and the eventually correction of the system state for the safe systems operation near their technical limit thereby supporting the Nigerian 330kv transmission system

operators from overloading of the transmission system paths. Overloading of Nigerian 330kv transmission network have caused a lot of blackout across the country in the time past because the Nigerian 330kv transmission lines are operating under heavily loaded condition even in congested state for economical operation couple with the high electricity demand in the country with low power generation and deregulated environment there is a chance of loss of this Nigerian 330kv transmission line due to fault. At each operating point instant, these tools should permit to know if the regnant operating point is safe (Agbontaen, *et al.,* 2019). The tools function should be the calculation of the margin to a defined power transfer capacity limit of the 330kv transmission system and active in voltage stability quantification of the power system transfer amount. With this urgent monitoring tool, the need for the adoption of smart grid technologies which will serve as an active monitoring tool that can savage Nigerian 330kv transmission system monitoring flux became more urgent.

There are three system theoretical limits which situation awareness is paramount during the power system operation which require continuous and conjointly monitoring of all these limits. The system theoretical limits include: power system stability, power system outage security and power system short circuit. Though in this work, we are focusing majorly on the power system stability.

PV curves are plots of load bus voltage magnitudes against load active power for a given power factor. The extremes of PV curves (nose points) are found by load flow calculations where the distance between the current operating points and the extremes is the stability criterion. PV curves give the proximity of voltage collapse points. Loading margin of a power system can be determined using P-V curves of a power system at a particle operating point with two solution points (Samuel, 2017).

II. REVIEW OF RELATED WORKS

Parul and Dharmeshkumar (2013) proposed voltage stability assessment using continuation power flow method. In their research, it showed how much the system is close to voltage stability. P-V curve of the system which gives maximum loading of the system was obtained using continuation power flow method. For continuation power flow, power system analysis toolbox was used. Continuation power flow method is a predictor, corrector scheme which find the solution. In terms of the simulation, IEEE 14 bus system was taken. The system was run into 2 different conditions; with and without considering generator power limits. Bifurcation point was the point the continuation power flow was run up to and after reaching the maximum loading point, it stops. In this method, voltage stability margin can easily be found and the weakest bus can also be found out by applying further calculation. Optimization technique to determine the static voltage stability, load flow and continuation power flow in the analysis of voltage stability uses three bus system and IEEE 14 bus system. The main analysis parameters which determine the voltage stability margin or loading margin of the system are continuation power flow and optimization technique. Successive power flow solution to calculate the voltage profile up to the collapse point is computed by continuation power flow. Optimization technique gives solution only at optimal point but with more accurate solution. Optimization toolbox is used for load flow in MATLAB.

Althowibi and Mustafa (2013) proposed power system voltage stability: Indication, allocations and voltage collapse predictions. Four indices were used for the voltage stability in the transmission line and system buses. For the study of dynamics of load and generator, two indices were used for the system buses termed as VPI_{bus} and $VQI_{bus.}$ For the study of transmission stress and outages, the remaining two indices VPI_{line} and VQI_{line} were used for transmission line voltage stability. These indices are fast, accurate and provide the information about maximum active and reactive power transfer in the system. This analysis is done on the IEEE 14 bus system and IEEE 118 bus system. The analytical result obtained from the indices helps to avoid voltage collapse and prevent the system from voltage instability.

Ezekiel and Engala (2019) proposed enhancing the voltage stability of the Nigeria 330KV 48 bus power system network using modal/eigenvalue analysis. The study is based on the application of modal analysis on the 48 bus 330KV Nigerian network using PSAT MATLAB Toolbox. The Modal/Eigenvalue analysis

technique was used to investigate the stability of the 48 bus Nigeria power network system. The modal method calculates the smallest eigenvalue and all the associated eigenvectors of the Jacobian matrix using the steady state mode. The magnitude of the smallest eigenvalue estimates the proximity of the system to the voltage instability. The participation factor can be employed to identify the bus that provides the highest contribution to the instability of the system. The 48 bus Nigerian network was simulated under static loads and changing loads and modal/eigenvalue analysis was performed on the system under each of these conditions. It was found that increase in loads at the three selected weakest buses reduced the stability of the system. Results obtained in the study proved that reactive power compensators were able to drastically improve the stability profile of the 48 bus Nigeria network and even rescue the system at the event of voltage instability especially the ones caused by change in loads.

Adepoju *et al.* (2017) proposed application of static synchronous series compensator (SSSC) to the 330KV Nigeria transmission network for voltage control. According to them, longitudinal power systems of Nigerian 330KV transmission network have steady state problems of congestion, voltage limit violation and high active power loss. That static synchronous series compensator (SSSC) currently in use for solving mesh problems has not been applied to Nigeria 330KV power network. He then propose it that the work involves the use of SSSC for solving problems associated with Nigeria 330KV longitudinal power network using voltage magnitude as performance metrics. Steady state modeling of power system and SSSC modeling produced two sets of non-linear algebraic equations that were solved simultaneously using Newton-Rapson algorithm (NR) method and was implemented using MATLAB. His results of power flow analysis of Nigeria 330KV transmission network without SSSC showed that, there was voltage limit violation of ± 10% at bus 16 Gombe (0.8973p.u.) however, the results with incorporation of SSSC showed that, the SSSC was effective in eliminating voltage limit violation, control bus voltage magnitude to specified value (bus 14 from 0.9462p.u. to 1.00p.u.) and reduced network active power loss by more than 5% of base case (93.87MW). Therefore, SSSC is effective in solving steady-state problems of longitudinal power systems.

Madueme *et al.* (2015) proposed simulation modeling of voltage stability of an interconnected electric power system network. The study was achieved by modeling the existing interconnected power system using power system analysis tools (PSAT). THE IEEE 14 bus system and the Nigeria 330KV, 30 buses uncompensated and compensated power system were modeled in a digital computer using NEPLAN software operated in MATLAB 7.5.0 environment. With the known parameters of the network, the system is simulated for investigation and assessment of voltage stability. Modal/eigenvalue analysis was used with voltage reactive power sensitivity used as a determining factor while the Q-V curves were used to confirm the result. The values of the various eigenvalues are used for the determining of the various V-Q sensitivities of the buses, and the value of the least eigenvalue is used to indicate the bus at that value that will on loading experience voltage collapse. The highest positive V-Q sensitivity indicates the proximity to voltage collapse with the increased loading of the bus. The modeled networks on simulation gave load flow results to voltages within acceptable ranges (± 5%) for the IEEE 14 bus system and the compensated Nigerian system except three nodes for the uncompensated.

III. MATERIALS AND METHOD

3.1 Load Flow Analysis Using Newton Rapson Method

Considering an n-bus power system shown in Figure 3.1 below;

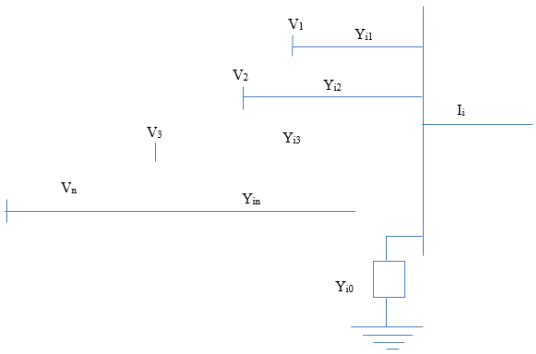

Figure 3.1: Power System Bus

Applying Kirchhoff's Current Law to bus I;

$$I_i = Y_{i0}V_i + Y_{i1}(V_i - V_1) + Y_{i2}(V_i - V_2) + Y_{i3}(V_i - V_3) + \ldots\ldots + Y_{in}(V_i - V_n) \quad (3.1)$$

$$= (Y_{i0} + Y_{i1} + Y_{i2} + Y_{i3} + \ldots\ldots + Y_{in})V_i - Y_{i1}V_1 - Y_{i2}V_2 - Y_{i3}V_3 - \ldots\ldots - Y_{in}V_n$$

Thus; $I_i = V_i \sum_{k=0}^{n} Y_{ik} - \sum_{k=1}^{n} Y_{ik}V_k \ , \ k \neq i \quad (3.2)$

The real and reactive power at bus I is given as;

$$S_i = P_i + jQ_i = V_i I_i^* \quad (3.3)$$

$$I_i = \frac{S_i^*}{V_i^*} = \frac{P_i - jQ_i}{V_i^*} \quad (3.4)$$

Using equation (3.4) to substitute into equation (3.2) gives;

$$\frac{P_i - jQ_i}{V_i^*} = V_i \sum_{k=0}^{n} Y_{ik} - \sum_{k=1}^{n} Y_{ik}V_k \ , \ k \neq i \quad (3.5)$$

or

$$P_i - jQ_i = V_i^* \sum_{k=0}^{n} V_i Y_{ik} - V_i^* \sum_{k=1}^{n} Y_{ik}V_k \ , \ k \neq i \quad (3.6)$$

Equation (3.6) may be written as

$$P_i - jQ_i = V_i^* \sum_{k=1}^{n} Y_{ik}V_k \ , \ k \neq i \quad (3.7)$$

Equation (3.7) is the resultant mathematical formulation for load flow problems analyzed above which resulted in a solution of nonlinear algebraic equations and can only be solved by applying iterative methods. In this thesis, Newton-Raphson method is applied to the solution in a polar form because it results in a smaller number of equation derivations, added with its quadratic convergence property and ability to handle large power network.

Since the n power flow equations (Eq. 3.6) are complex, let the bus voltages and admittance be written in polar form;

$$\begin{aligned} V_i &= |V_i| e^{j\delta_i} \\ V_i^* &= |V_i| e^{-j\delta_i} \\ V_k &= |V_k| e^{j\delta_k} \\ Y_{ik} &= |Y_{ik}| e^{j\theta_{ik}} \end{aligned} \quad (3.8)$$

Where;

δ : is the phase angle of the bus voltages and θ_{ik} is the admittance angle

From Eq. (3.8), substituting the values of V_i^* , V_k , Y_{ik} into Eq. (3.7) and equating the real part and the imaginary part yields;

$$P_i = \sum_{\substack{k=1 \\ k \neq i}}^{n} |V_i||Y_{ik}||V_k| \cos(\theta_{ik} - \delta_i + \delta_k) \quad (3.9)$$

$$Q_i = -\sum_{\substack{k=1 \\ k \neq i}}^{n} |V_i||Y_{ik}||V_k| \sin(\theta_{ik} - \delta_i + \delta_k)$$

$$for\ i = 2,3,4,5,\ldots\ldots n\ because bus 1 is\ taken\ as\ slack\ bus \quad (3.10)$$

Load flow equations (3.9) and (3.10) above are solutions of nonlinear algebraic equations, two equations (real part P_i and imaginary part Q_i) at each bus. If the slack bus (bus 1) is excluded then, V and δ is specified and remains fixed throughout, the total number of equations to be calculated for n bus system becomes $(2n-1)$ equations.

The load flow equations using Newton-Raphson jacobian matrix becomes

$$\begin{bmatrix} \Delta P_2^r \\ \\ \\ \Delta P_3^r \\ \vdots \\ \vdots \\ \Delta P_n^r \\ \\ \cdots \\ \\ \Delta Q_2^r \\ \\ \\ \Delta Q_3^r \\ \\ \vdots \\ \vdots \\ \\ \Delta Q_n^r \end{bmatrix} = \begin{bmatrix} & & & & & & & & \\ & & & & & & & & \end{bmatrix} \begin{bmatrix} \Delta \delta_2^r \\ \\ \\ \Delta \delta_3^r \\ \vdots \\ \vdots \\ \Delta \delta_n^r \\ \\ \cdots \\ \\ \Delta |V_2|^r \\ \\ \\ \Delta |V_3|^r \\ \\ \vdots \\ \vdots \\ \\ \Delta |V_n|^r \end{bmatrix}$$

(3.13)

Therefore;

$$\begin{bmatrix} \Delta P_i^r \\ \\ \cdots \\ \\ \Delta Q_i^r \end{bmatrix} = \begin{bmatrix} \Delta P_2^r \\ \\ \Delta P_3^r \\ \\ \Delta P_n^r \\ \cdots \\ \Delta Q_2^r \\ \\ \Delta Q_3^r \\ \\ \Delta Q_n^r \end{bmatrix} \text{ and}$$

$$\begin{bmatrix} \Delta \delta^r \\ \\ \cdots \\ \\ \Delta |V|^r \end{bmatrix} = \begin{bmatrix} \Delta \delta_2^r \\ \\ \Delta \delta_3^r \\ \\ \Delta \delta_n^r \\ \cdots \\ \Delta |V_2|^r \\ \\ \Delta |V_3|^r \\ \\ \Delta |V_n|^r \end{bmatrix} \quad (3.11)$$

In order to compute the elements of the jacobian matrix (J), Equation (3.10) can be written as

$$\begin{bmatrix} \Delta P^r \\ \cdots \\ \Delta Q^r \end{bmatrix} = \begin{bmatrix} J_1^r & \vdots & J_2^r \\ \cdots & \vdots & \cdots \\ J_3^r & \vdots & J_4^r \end{bmatrix} \begin{bmatrix} \Delta \delta^r \\ \cdots \\ \Delta |V|^r \end{bmatrix} \quad (3.12)$$

The elements of the sub-matrices (J_1^r, J_2^r, J_3^r *and* J_4^r) becomes

The diagonal element of J_1 is

$$\frac{\partial P_i}{\partial \delta_i} = \sum_{\substack{k=1 \\ k \neq i}}^{n} |V_i||V_k||Y_{ik}| \sin\left(\theta_{ik} - \delta_i + \delta_k\right) \quad (3.13)$$

The off-diagonal element of J_1 is

$$\frac{\partial P_i}{\partial \delta_k} = -|V_i||V_k||Y_{ik}| \sin\left(\theta_{ik} - \delta_i + \delta_k\right) \quad (3.14)$$

The diagonal element of J_2 is

$$\frac{\partial P_i}{\partial |V_i|} = 2|V_i||Y_{ik}| \cos\theta_{ii} + \sum_{\substack{k=1 \\ k \neq i}}^{n} |V_k||Y_{ik}| \cos\left(\theta_{ik} - \delta_i + \delta_k\right)$$

(3.15)

The off-diagonal element of J_2 is

$$\frac{\partial P_i}{\partial |V_m|} = |V_i||Y_{ik}|\cos(\theta_{ik} - \delta_i + \delta_k) \quad (3.16)$$

The diagonal element of J_3 is

$$\frac{\partial Q_i}{\partial \delta_i} = \sum_{\substack{k=1 \\ k \neq i}}^{n} |V_i||V_k||Y_{ik}|\cos(\theta_{ik} - \delta_i + \delta_k) \quad (3.17)$$

The off-diagonal element of J_3 is

$$\frac{\partial Q_i}{\partial \delta_k} = -|V_i||V_k||Y_{ik}|\cos(\theta_{ik} - \delta_i + \delta_k) \quad (3.18)$$

The diagonal element of J_4 is

$$\frac{\partial Q_i}{\partial |V_i|} = 2|V_i||Y_{ik}|\sin\theta_{ii} - \sum_{\substack{k=1 \\ k \neq i}}^{n} |V_k||Y_{ik}|\sin(\theta_{ik} - \delta_i + \delta_k) \quad (3.19)$$

The off-diagonal element of J_4 is

$$\frac{\partial Q_i}{\partial |V_m|} = -|V_i||Y_{ik}|\sin(\theta_{ik} - \delta_i + \delta_k) \quad (3.20)$$

The power residues $(\Delta P_i^r \text{ and } \Delta Q_i^r)$ can be determined as the difference between the specified and computed values as follows;

$$\Delta P_i^r = P_i^{SPd} - P_i^r \quad (3.21)$$

$$\Delta Q_i^r = Q_i^{SPd} - Q_i^r \quad (3.22)$$

Where, $P_i^{SPd} \text{ and } Q_i^{spd}$ are the power specified while $P_i^r \text{ and } Q_i^r$ are the power calculated with the latest determined values of bus voltage at any iteration r (r is an iteration count)

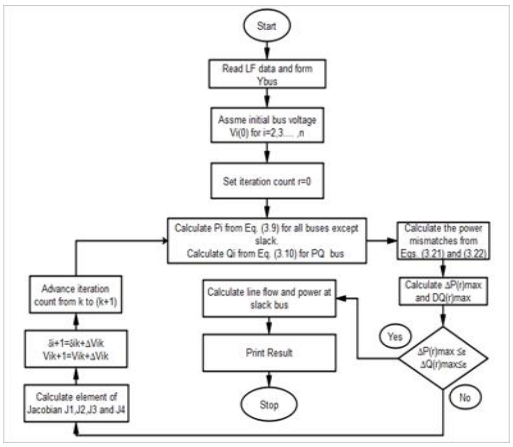

Figure 3.2: Flow-Chart for Load Flow Solution Using N-R Method (Source: Gupta, 2005).

3.2 Optimal Placement of the Static Var Compensator

Newton Rapson load flow method was employed to determine optimal locations (buses) for static var compensator placement in the system. This method is systematic procedures for optimal placements that regulate voltages between there limits and inject reactive power for those candidate buses. The transmission line voltages are required to maintain within $\pm 5\%$ of the rated voltage for upper and lower limits after optimal placement of the SVC. The optimal placement of SVC on the right locations ensures that no voltage constraints would be violated once a second load flow is performed using NEPLAN software.

So the optimal locations identified for SVC placement are shown in table 4.1 which are; (Maiduguru bus, Jalingo bus, Yola bus, Damaturu bus and Gombe bus). Its worth noting that SVC is shunt connected FACTS device, meaning it is installed in parallel with a bus.

3.3 P-V Curve Modeling

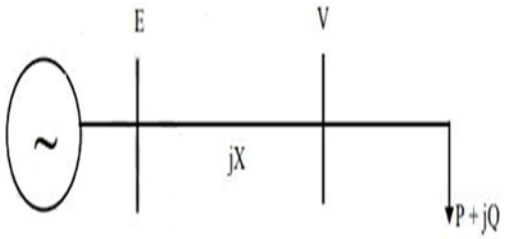

Figure 3.8: A single line diagram of a two bus system

Transmission line resistance real and reactive being neglected, the powers are given by the equations 3.56 and 3.57

$$P = \frac{EV}{X} Sin\delta \quad (3.56)$$

$$Q = \frac{EV}{X} Cos\delta - \frac{V^2}{X} \quad (3.57)$$

P-V curves show the relationship between the load in MW in a particular area and the bus voltage for different power factors (where $\tan\phi = \frac{Q}{P}$) as the load angle is not considered for this study, then it can be eliminated.

Let $p = \frac{PX}{E^2},\ q = \frac{QX}{E^2}\ and\ \ v = \frac{V}{E}$

Normalizing the (3.56) and (3.57) based on the short circuit power

$$S = \frac{E^2}{X}$$

We obtain

$$p = vSin\delta \quad (3.58)$$

$$q = vCos\delta - v^2 \quad (3.59)$$

Load angle δ can be eliminated

By assuming resistive load i.e $\tan\phi = \frac{Q}{P} = 0\ \ as\ \ Q = 0$

Using identity

$$v^2 = v^2Cos^2\delta + v^2Sin^2\delta$$

$$vSin\delta = \sqrt{v^2 - v^2Cos^2\delta}$$

From transform equation (3.58) and (3.59)

$$p = vSin\delta = \sqrt{v^2 - v^2Cos^2\delta} \quad and\ \ q = vCos\delta - v^2$$

$$p = \sqrt{v^2 - (q + v^2)^2} \quad (3.60)$$

$$\text{Because } Q = 0;\ \ q = \frac{QX}{E^2} = 0$$

$$p = \sqrt{v^2 - v^4} \quad (3.61)$$

The above relationship is used to plot the p-v curve

IV. RESULTS AND DISCUSSION

4.1 Nigerian 48 bus Improved Network

NEPLAN software simulation result of the improved 330kv transmission network is presented in figure 4.1 below. All the buses in green color signify stability state of the system.

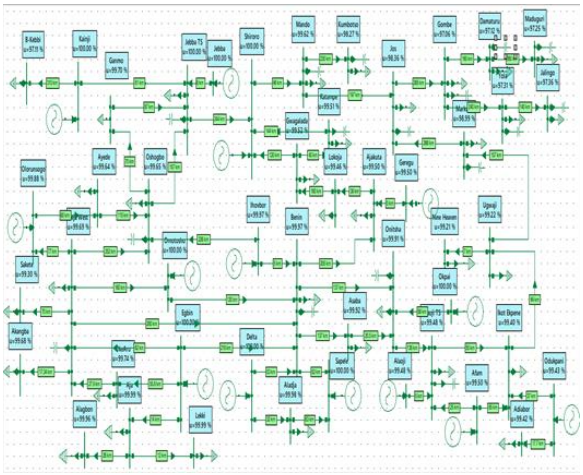

Figure 4.1: Post-Upgrade Networks Simulation in NEPLAN Software

4.2 Improved Buses Result

The improved vulnerable buses NEPLAN simulation result is presented in figure 4.2 below showing the improved operating voltages and the system power flow as contained and declared by statutory condition. The buses displaying green color signifies stability of the system.

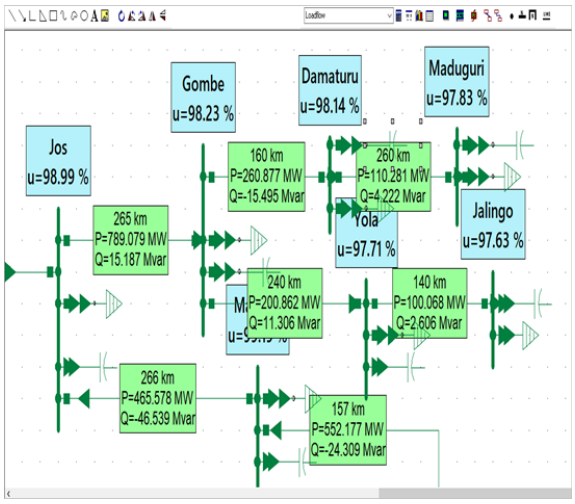

Figure 4.2: Improved Buses Network Simulation in NEPLAN Software

4.3 Bus Operating Voltage for Nigerian 330KV Transmission Network

Table 4.1 below shows the 48 bus nominal voltages and the improved bus operating voltages of the system for Nigerian 330KV network.

Table 4.1: Bus Operating Voltage for Post-Upgrade Network Condition

No	Bus Name	Nominal (kV)	Post- Upgrade (KV)	Post- Upgrade (P.U.)	Post- Upgrade (%)
1	Adiabor	330	328.581	0.9957	99.57
2	Afam	330	328.779	0.9963	99.63
3	Aja	330	329.967	0.9999	99.99
4	Ajakuta	330	328.35	0.995	99.50
5	Akangba	330	328.944	0.9968	99.68
6	Aladja	330	329.934	0.9998	99.98
7	Alagbon	330	329.868	0.9996	99.96
8	Alaoji	330	328.746	0.9962	99.62
9	Alaoji TS	330	328.746	0.9962	99.62
10	Asaba	330	329.769	0.9993	99.93
11	Ayede	330	328.812	0.9964	99.64
12	Benin	330	329.901	0.9997	99.97
13	B-Kebbi	330	320.463	0.9711	97.11
14	Damaturu	330	323.862	0.9814	98.14
15	Delta	330	330	1.00	100.00
16	Egbin	330	330	1.00	100.00
17	Ganmo	330	329.01	0.997	99.70
18	Geregu	330	328.35	0.995	99.50
19	Gombe	330	324.159	0.9823	98.23
20	Gwagalada	330	328.416	0.9952	99.52
21	Ihovbor	330	329.901	0.9997	99.97
22	Ikeja West	330	328.977	0.9969	99.69
23	Ikot Ekpene	330	328.515	0.9955	99.55
24	Jalingo	330	322.179	0.9763	97.63

25	Jebba	330	330	1.00	100.00
26	Jebba TS	330	330	1.00	100.00
27	Jos	330	326.667	0.9899	98.99
28	Kainji	330	330	1.00	100.00
29	Katampe	330	328.383	0.9951	99.51
30	Kumbotso	330	324.489	0.9833	98.33
31	Lekki	330	329.967	0.9999	99.99
32	Lokoja	330	328.218	0.9946	99.46
33	Maiduguri	330	322.839	0.9783	97.83
34	Mando	330	328.911	0.9967	99.67
35	Markudi	330	327.459	0.9923	99.23
36	New Heaven	330	327.921	0.9937	99.37
37	Odukpani	330	328.581	0.9957	99.57
38	OkeAro	330	329.142	0.9974	99.74
39	Okpai	330	330	1.00	100.00
40	Olorunsogo	330	329.604	0.9988	99.88
41	Omotosho	330	330	1.00	100.00
42	Onitsha	330	329.736	0.9992	99.92
43	Oshogbo	330	328.845	0.9965	99.65
44	Sakete	330	327.69	0.993	99.30
45	Sapele	330	330	1.00	100.00
46	Shiroro	330	330	1.00	100.00
47	Ugwaji	330	327.921	0.9937	99.37
48	Yola	330	322.443	0.9771	97.71

Table 4.1 shows the nominal and operating voltage of the system for post-upgrade network condition. The post-upgrade network condition is the state when static var compensators are installed. Table 4.3 shows that no buses violate the statutory limit condition of 0.95p.u. (313.5kV) - 1.05p.u. (326.5kV).

4.4 Voltage Profile and Bus Number for Post-Upgrade Network Condition

Figure 4.3 below shows voltage profile of the system for bus nominal voltage and the improved bus operating voltages against bus number.

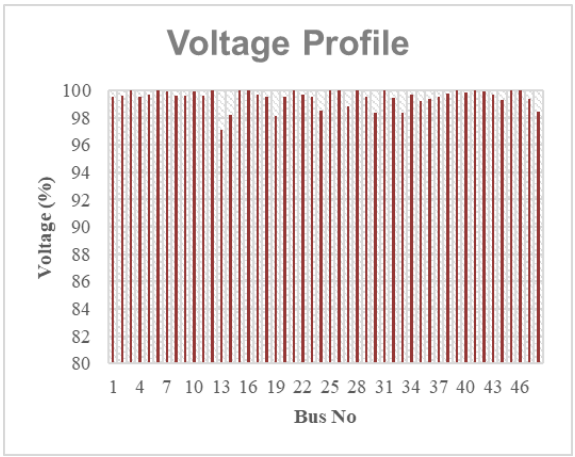

Figure 4.3: Voltage Profile for Post-Upgrade Network Condition

Figure 4.3 above depicts the voltage maximum loadability of the post-upgrade network. The variation

of load is because of the different operating state of the bus voltages and the 5 vulnerable buses are seen to be compensated and improved via optimal static var placement. All the buses are above 96% showing that the buses are stable.

4.5 Bus Voltage Improvement

Figure 4.4 depicts the vulnerable buses voltage improvement achieved, signifying improved voltage loadability of the system. Hence, the system voltage stability also improved.

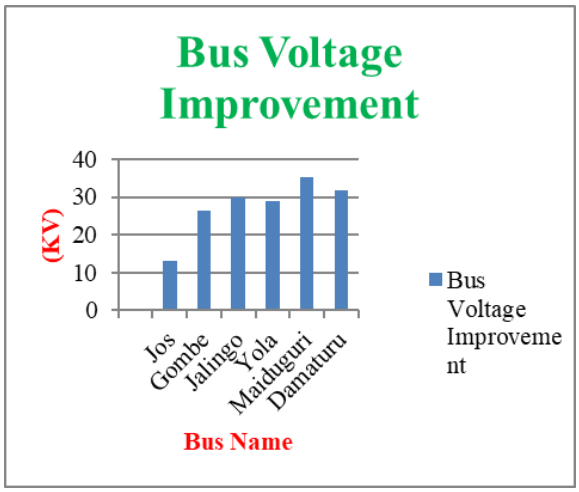

Figure 4.4: Bus Voltage Improvement

The graph shows the improvement achieved after optimal placement of static var compensator on the vulnerable buses and also showcases the maximum voltage loadability of the buses. The maximum voltage loadability improvement achieved is above 10KV.

4.6 P-V Curve Comparison for Voltage (%) and Real Power (MW)

P-V curve comparison for maximum loading (operating margin) of pre-upgrade, post-upgrade and ANN respectively in respect to Maiduguru bus, Jalingo bus, Yola bus, Damaturu bus and Gombe. The result shows how the curves analyses the effect of real and reactive power change on the 5 buses. The slope and the operating point of the curves were employed as an indicator for determining voltage security. Similarly, the curves provide critical voltage and real power distance to voltage collapse as a measure for system robustness and also the improvement achieved.

4.6.1 P-V Curve Comparison Plot for Gombe Voltage (%) and Real Power (MW)

Figure 4.5 shows the P-V curve comparison plot for Gombe bus voltage (%) against real power (MW). The curve analyses the effect of real and reactive power change on Gombe, bus.

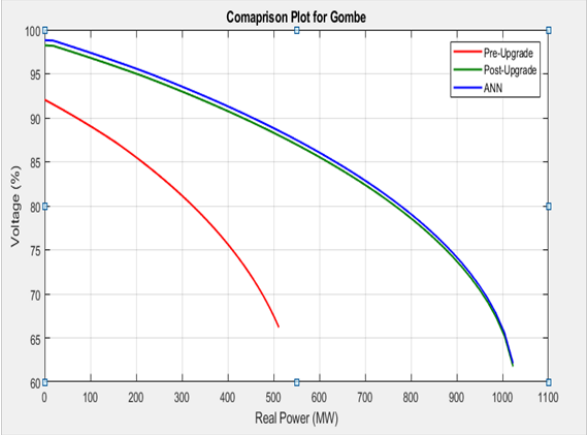

Figure 4.5: P-V Curve Comparisons for Gombe Bus

Figure 4.5 show that the red curve depicts Gombe bus maximum loadability of the pre-upgrade network at 550MW. The green curve indicates the effect of static var compensation with maximum loadability at 1020MW. Therefore, the improvement achieved is 470MW. Finally, the ANN technique is represented by the blue curve and it validated the improvement achieved as the voltage and real power remain fairly constant with static compensators.

4.6.2 P-V Curve Comparison Plot for Jalingo Voltage (%) and Real Power (MW)

Figure 4.6 shows the Jalingo bus comparison plot. The curve analyses the effect of real and reactive power change on Jalingo bus.

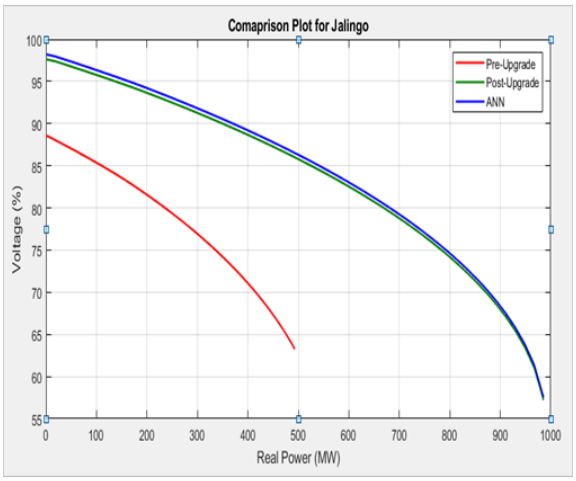

Figure 4.6: P-V Curve Comparisons for Jalingo Bus

Figure 4.6 show that the red curve depicts the maximum loadability of the bus in pre-upgrade network at 550MW. The green curve indicates the effect of static var compensation with maximum loadability at 1000MW. Therefore, the improvement achieved is 450MW. Finally, the ANN technique is represented by the blue curve and it validated the improvement achieved as the voltage and real power remain fairly constant with static compensators.

4.6.3 P-V Curve Comparison Plot for Yola Voltage (%) and Real Power (MW)

Figure 4.7 shows the Yola bus comparison plot. The curve analyses the effect of real and reactive power change on Yola bus.

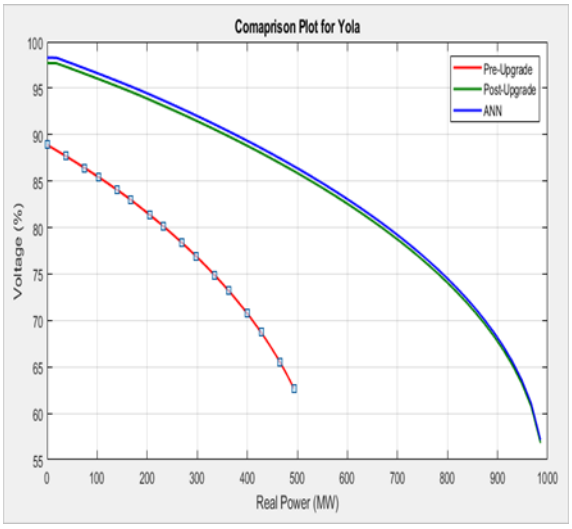

Figure 4.7: P-V Curve Comparisons for Yola Bus

Figure 4.7 show that the red curve depicts the maximum loadability of the bus in pre-upgrade network at 580MW. The green curve indicates the effect of static var compensation with maximum loadability at 990MW. Therefore, the improvement achieved is 410MW. Finally, the ANN technique is represented by the blue curve and it validated the improvement achieved as the voltage and real power remain fairly constant with static compensators.

4.6.4 P-V Curve Comparison Plot for Maiduguri Voltage (%) and Real Power (MW)

Figure 4.8 shows the Maiduguri bus comparison plot. The curve analyses the effect of real and reactive power change on Maiduguri, bus.

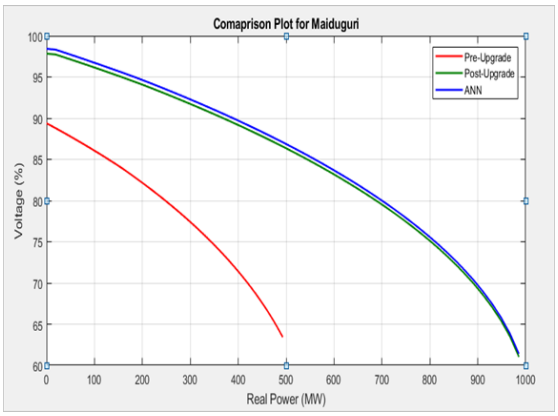

Figure 4.8 P-V Curve Comparisons for Maiduguri Bus

Figure 4.8 show that the red curve depicts the maximum loadability of the bus in pre-upgrade network at 520MW. The green curve indicates the effect of static var compensation with maximum loadability at 1000MW. Therefore, the improvement achieved is 480MW. Finally, the ANN technique is represented by the blue curve and it validated the improvement achieved as the voltage and real power remain fairly constant with static compensators.

4.6.5 P-V Curve Comparison Plot for Damaturu Voltage (%) and Real Power (MW)

Figure 4.9 shows the Damaturu bus comparison plot. The curve analyses the effect of real and reactive power change on Damaturu bus.

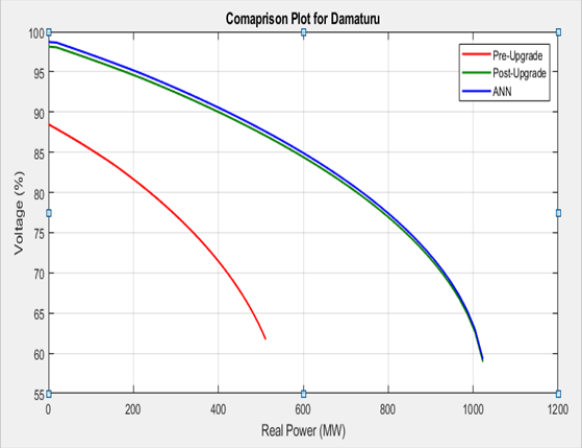

Figure 4.9 P-V Curve Comparisons for Damaturu Bus

Figure 4.9 show that the red curve depicts the maximum loadability of the bus in pre-upgrade network at 570MW. The green curve indicates the effect of static var compensation with maximum loadability at 1050MW. Therefore, the improvement achieved is 480MW. Finally, the ANN technique is represented by the blue curve and it validated the improvement achieved as the voltage and real power remain fairly constant with static compensators.

CONCLUSION

Following the completion of the research, it can be observed that the research successfully addressed the objectives set out at the beginning of the research. Maximum loadability of the system was recorded via P-V curve plot and artificial neural network added to the plot to validate the improvement achieved.

REFERENCES

[1] Ademola, A., Aremu, A. C., Isaac, A. S., & Ayoade, F. A. (2016). Contingency analysis for assessing line losses in Nigerian 330-kv power lines. *International journal of engineering and advanced technolog*, 5(3), 66-78.

[2] Adepoju, G. A., Sanusi, M. A., & Tijani, M. A. (2017). Application of SSSC to the 330kv Nigerian transmission network for voltage control. *Nigerian Journal of Technology (NIJOTECH)*, *36*(4), 1258 – 1264.

[3] Agbontaen, F. O., Egwaile, J. O., & Okakwu, I. (2019). Power flow analysis of the enhanced proposed 330kv transmission network of the Nigeria grid. *Mehran university research journal of engineering & technology*, 38(4), 875-884.

[4] Althowibi, F. A., & Mustafa, M. W. (2013). Power system voltage stability: Indications, allocations and voltage collapse predictions. *International journal of advanced research in electrical, electronics and instrumentation engineering*, 2(7), 12–15.

[5] Ezekiel, N. A., & Engla, A. (2019). Enhancing the voltage stability of the Nigerian 330kv 48-bus power system network using modal/eigenvalue analysis. *Journal of Information Engineering and Applications*, 9(7), 2224-5782. www.iiste.org

[6] Gupta, J. B. (2013). *A course in power system* (2nd ed.). Chand Publication, 62-65.

[7] Madueme, T. C., & Kalu, O. O. (2015). *Application of artificial neural network for enhanced power systems protection on the Nigerian 330KV network*. [Master Degree Disertation, University of Nigeria, Nsukka], 93-96. Researchgate.net.

[8] Parul, U., & Dharmeshkumar, P. (2013). voltage stability assessment using continuation power flow method. *International journal of advanced research in electrical, electronic and instrumentation engineering*, 2(4), 22-25.

[9] Samuel, I. A. (2017). *A new voltage stability index for predicting voltage collapse in electrical power system networks.* [Doctoral thesis, Covenant University, Ota Ogun State Nigeria], *74-80.* Researchgate.net.